

Mathematical Modelling of Radiating Processes in the Solids Irradiated by Heavy Ions

Sh.E. Jeleunova*, T.A.Shmygaleva, A.I.Kupchishin, E.V.Shmygalev, A.A.Kupchishin,
L.Sh.Cherikbayeva, I.D.Masyrova, and B.B.Alrakymov

Al-Farabi Kazakh National University,
Al-Farabi 71, 050040 Almaty, Kazakhstan
{Shmyg1953}@mail.ru

Abstract. In this work the modelling of the processes of radiation defect formation in solids irradiated by heavy ions within the cascade-probabilistic method (CPM), which is analytic. All the mathematical models describing these processes are received both from physical reasons, and from Kolmogorov-Chapman equations. Essence of CPM consists in reception and further use cascade-probabilistic functions (CPF), CPF makes sense of the fact that the particle generated on depth h' will reach depth h after N number of impacts. Mathematical models are received in such a way that in them are considered energy losses to ionization and excitation of the electron envelopes of the atoms of medium with interaction of heavy ions with solid.

Keywords: modeling, defect formation, cascade-probabilistic, ion, target, recurrence relation, approximation, concentration, vacancies cluster, spectrum of primarily knocked-on atoms.

Introduction

Charged particle along the path of its motion continuously loses its energy for the ionization and excitation (the energy losses of dE/dx for each type of particles depending on energy they are known and described by analytical expressions, in particular, by Bethe-Bloch formula). Collisions with the atoms, the nuclei occur discretely. After collisions, primary particles preserve direction of their motion. During the motion of the charged ions through the substance their run depends on the energy through the section interaction of $\lambda(E) = 1/\sigma(E) * n$, where n - number of atoms in the cubic centimeter of medium. The mathematical model of cascade-probabilistic functions taking into account energy losses for the ions with the use of recurrence relations in accordance with this physical model is developed.

Further the analysis of CPF calculations is carried out in the dependence on the number of interactions and depth of penetration of particles and the new regularities are obtained, appearing with interaction of heavy ions with solids. The features of these functions are analyzed. It is shown that, in spite of apparent simplicity, their calculation on PC it is often difficult, it is necessary to have recourse to different mathematical devices, to use special methods, to select the real region of finding the result. The detailed analysis of behavior of these functions depending on energy of flying particles, atom number of a target, depth of generation and registration, number of interactions is carried out also.

The successfully selected approximated formulas for a number of the parameters contributed to obtaining of CPF in the analytical form, which made it possible considerably to more deeply understand general regularities of the processes. The received CP - functions were used for calculating of PKA spectra and concentration of vacancies clusters, formed during irradiation solids by heavy ions (1-1000 keV). New regularities are revealed during calculations, for the concentration of vacancies clusters it is also necessary to match the real region of finding the result. As show calculations, these results sufficiently well will agree with existing experimental data. Work was carried out in the context of CPF [1-6].

Passage of ions through substance is a complex task as at creation physical and mathematical models. The set of types of flying particles and targets of Periodic system of Mendeleev represents huge quantity of elements. Thus it is possible to consider various situations when the mass number of flying particles less than atomic number of a target, is commensurable with atomic number of a target and a case when the atomic weight of a flying particle is more or much more than atomic number of a target. Elements are classified by us on easy and heavy on the density of element.

Recurrence relations from which in cascade-probabilistic functions are deduced, turn out from Kolmogorov-Chapman equation for Markov process, which has a following form [7]:

$$p_{in}(\tau, t) = \sum_{\nu} p_{i\nu}(\tau, s) p_{\nu n}(s, t), \quad (1)$$

where $\tau < s < t$.

From (1) it is received

$$\psi_{in}(h', h, \alpha_0) = \sum_{\nu} \psi_{i\nu}(h', h'', \alpha_0) \psi_{\nu n}(h'', h, \alpha_0). \quad (2)$$

As process of interaction of ions with the solid is continuous on time and consequently, and on depth of penetration, the sum sign in expression (2) is replaced with integral. The following recurrence relation turns out:

$$\psi_n(h', h, E_0) = \int_{h'}^h \psi_{n-1}(h', h'', E_0) \psi_0(h'', h, E_0) * \sigma(h) dh'' . \quad (3)$$

As the integral isn't taken analytically as section Rezerford entering into sub-integral expression, has a complex form, the values calculated under formula Rezerford, are approximated by following expression [3]:

$$\sigma(h) = \sigma_0 \left(\frac{1}{\alpha(E_0 - kh)} - 1 \right), \quad (4)$$

then the recurrence relation will look as follows:

$$\begin{aligned} \psi_n(h', h, E_0) = \int_{h'}^h \psi_{n-1}(h', h'', E_0) \psi_0(h'', h, E_0) * \\ * \frac{1}{\lambda_0} \left(\frac{1}{\alpha(E_0 - kh'')} - 1 \right) dh'', \end{aligned} \quad (5)$$

where σ_0, α, E_0, k - coefficient of approximation, $\lambda_0 = 1/\sigma_0$.

From the given recurrence relation, we receive cascade-probabilistic functions in view of losses of energy as during interaction process of ions with the solid, there are losses of energy on ionization and excitation, which are necessary for considering turn out. The approximation expression includes energy that is constantly decreasing due to losses, run on the interaction also changes. Approximation is selected in such a way that the integral would be taken analytically, and so that the theoretical correlation ratio would be as close as possible to 1. Calculations were made in an interval of energy 100-1000 keV. Results of approximation are resulted in tables (1, 2) and in pictures 1, 2.

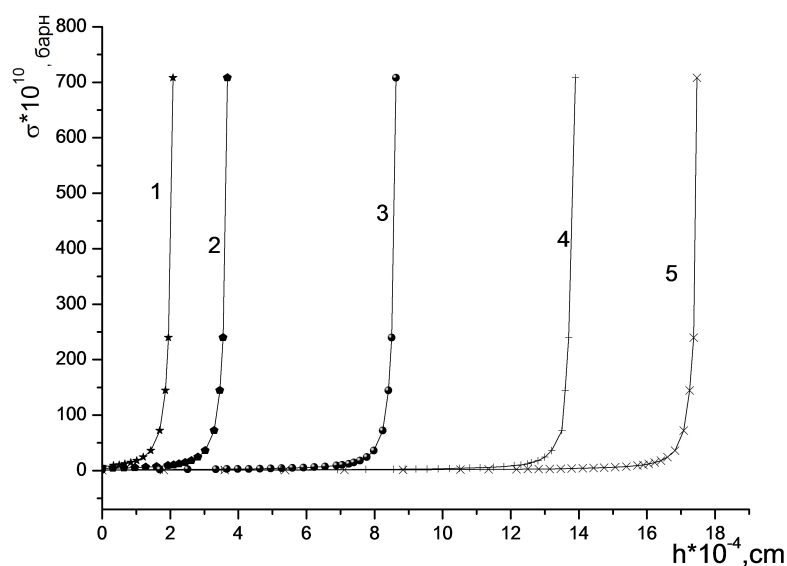
From charts and tables it is visible, that picked up approximation curves are described very well by rated data.

Table 1. Approximation parameters for gold in silicon

E_0	$\sigma_0 * 10^{10}$	a	E'_0	k	η
1000	3,3583	0,61385	0,91438	828,6	0,998
800	4,6131	0,86956	0,66608	735,34	0,994
500	6,0731	1,2172	0,41475	697,21	0,997
200	12,332	2,1647	0,18863	640,02	0,9996
100	16,961	2,8437	0,11084	626,72	0,9996

Table 2. Approximation parameters for gold in gold

E_0	$\sigma_0 * 10^{11}$	a	E'_0	k	η
1000	0,68122	0,71987	0,7813	24891	0,998
800	0,86517	0,99611	0,5655	21979	0,998
500	1,1304	2,4237	0,20356	11947	0,993
200	2,8258	3,5351	0,12891	14986	0,998
100	3,6475	1,2123	0,27707	53051	0,99992

**Fig. 1.** Approximation of section of cascade-probabilistic function for silver in silicon at $E_0 = 100(1), 200(2), 500(3), 800(4), 1000(5)$ keV. Points - the calculated data dependences of section on depth, a continuous line - approximation.

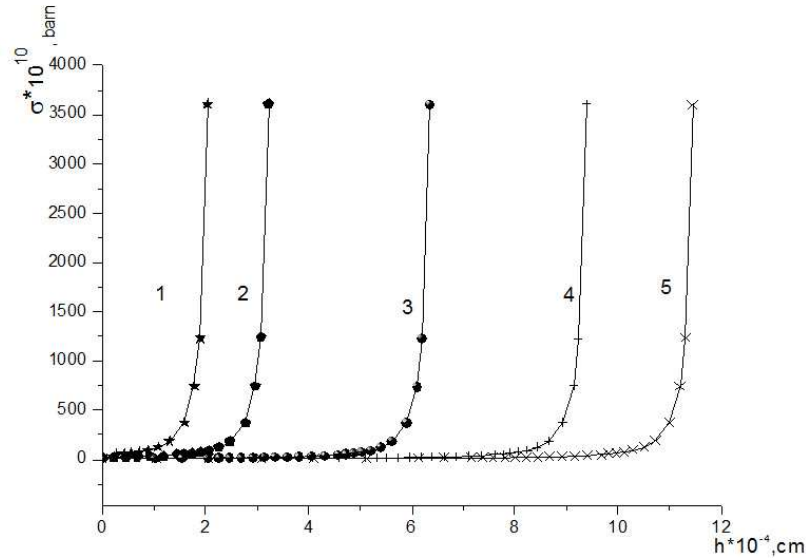


Fig. 2. Approximation of the modified section of cascade-probabilistic function for gold in silicon $E_0 = 100(1), 200(2), 500(3), 800(4), 1000(5)$ keV. Points - the calculated data dependences of section on depth, a continuous line - approximation.

From the recurrence relation (5) in cascade-probabilistic functions in view of losses of energy for ions in a following type are received [3]:

$$\psi_n(h', h, E_0) = \frac{1}{n! \lambda_0^n} \left(\frac{E_0 - kh'}{E_0 - kh} \right)^{-l} \exp \left(\frac{h - h'}{\lambda_0} \right) * \left[\frac{\ln \left(\frac{E_0 - kh'}{E_0 - kh} \right)}{ak} - (h - h') \right]^n. \quad (6)$$

However, to use this formula for calculations it is impossible, as at large values of number of impacts, or at small value 0 there is an overflow. The number of impacts for ions can reach some millions. Some algorithms are developed for calculation CPF.

In the given work to calculate the cascade-probabilistic functions depending on the number of interactions and the depth of penetration the following formula is used:

$$\psi_n(h', h, E_0) = \prod_{i=1}^n \left(\frac{\ln \left(\frac{E_0 - kh'}{E_0 - kh} \right) - (h - h')}{\lambda_0 i} \right) * \exp \left(\left(\frac{h - h'}{\lambda_0} \right) - \frac{1}{\lambda_0 ak} \ln \left(\frac{E_0 - kh'}{E_0 - kh} \right) \right), \quad (7)$$

where n - number of interactions, h', h - depths of generation and registration of the ion, λ_0, a, E_0, k - parameters of approximation. At a finding approximation parameters entering in (7), the following was used:

1. The section of atom-atom interactions was calculated by Rutherford's formula.
2. The depths of observations were located with the aid of the tables of the parameters of the spatial distribution of ion-implanted admixtures [8].
3. The calculated values of section were approximated by expression (4).

The results of CPF calculations depending on the number of interactions and depth of penetration of particles are presented in tables 3 - 6 and in figures 3, 4. The regularities arising at calculation CPF, spectra of the primarily knocked-on atoms and concentration of radiating defects are considered. In this case the influence of the depth of penetration, atomic number of a flying particle and target, initial energy of primary particle is considered. At CPF calculation in view of losses of energy for ions and concentration of radiating defects it is necessary to find actual area of a finding of result which behaves differently depending on various factors. For example, the area of CPF result calculated depending on number of interactions is narrowed and displaced to the left, from depth of penetration is narrowed and displaced to the right. It is especially necessary to note the case, when the density of the flying particle is great, and target it is small, then the selection of the boundaries of the region of result considerably is complicated. So at the end of the run of particle region strongly becomes narrow, sometimes to one hundredths of a percent, and curve can pass into the straight line. Therefore it is necessary to find area of result for flying heavy ions in easy and heavy elements and to reveal regularities of behavior of this area depending on initial energy of a primary particle, depth of penetration, atom number of the target.

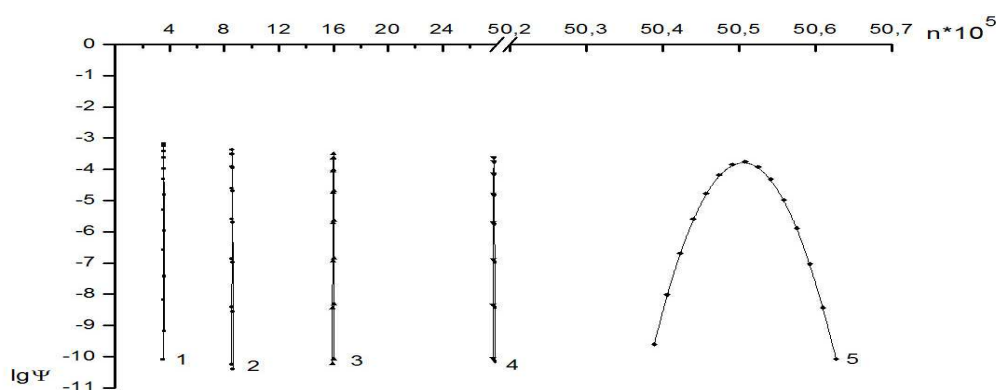


Fig. 3. Dependence of CPF on the number of interactions for gold in silicon with $h = 1, 2, 3, 4, 5 (\cdot 10^{-4})$; $E = 500$ keV (1-5).

Let's note some regularities of behavior of area of result at variation of number of interactions of particles:

1. With reduction of initial energy (a flying particle and a target the same) at the same depth the area of result is narrowed and displaced to the left.
2. Depending on depth of penetration behavior of area similar.
3. With an increase of atom number of the target depths of penetration decrease and reach $10^6 - 10^7$ cm., for example for gold in gold.
4. The narrowest area of result turns out at the big nuclear weight of a flying particle and small targets on the end of run and reaches the 100-th fractions of percent. In this case the count time strongly grows. For example, for gold in silicon with $E_0 = 1000$ MeV and $h = 0.001$ cm. the region of result becomes narrow to 0.017%.

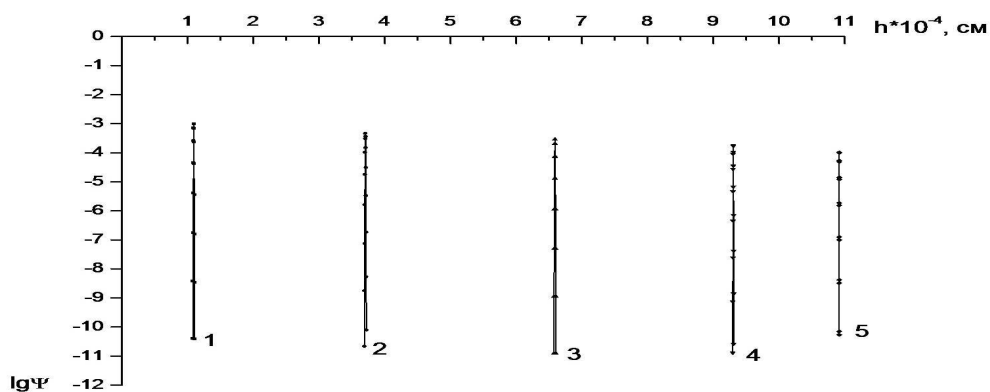


Fig. 4. Dependence of $\psi_n(h', h, E_0)$ on h for gold in silicon with $E_0=1000$ keV for $n = 161053; 728805; 1895427; 4551380; 13087291; (1-5)$.

Table 3. Dependence of the percentage of the shift of the left and right boundaries of the region of result on the number of interactions for gold in silicon: a) $E_0=1000$ keV; b) $E_0 = 500$ keV; c) $E_0 = 100$ keV

	$h * 10^4, \text{cm}$	$B_1, \%$	$B_2, \%$	N_n	$B_3, \%$
a)	1	10.9	-8	300	2,9
	3	25.98	-24.78	650	1,2
	5	39.5	-38.85	900	0,65
	7	53.03	-52.66	1250	0,37
	9	68.99	-68.81	1700	0,18
b)	$h * 10^4, \text{cm}$	$B_1, \%$	$B_2, \%$	N_n	$B_3, \%$
	1	16,18	-14,6	500	1,58
	2	29,15	-28,25	750	0,9
	3	41,63	-41,1	1000	0,53
	4	54,82	-54,52	1300	0,3
5	70,94	-70,795	1700	0,145	
c)	$h * 10^4, \text{cm}$	$B_1, \%$	$B_2, \%$	N_n	$B_3, \%$
	1	5,35	-2,75	350	2,6
	3	12,82	-11,5	650	1,32
	5	20,69	-19,85	800	0,84
	7	28,81	-28,2	1000	0,61
9	37,33	-36,9	1200	0,43	

Table 4. Dependence the percentage the displacement the left and right boundaries of the region of result from the number of interactions for gold in gold: a) $E_0 = 1000$ keV; b) $E_0 = 500$ keV; c) $E_0 = 100$ keV

a)	$h * 10^6, \text{cm}$	$B_1, \%$	$B_2, \%$	N_n	$B_3, \%$
	10	31,11	-27	180	4,11
	15	42,25	-39,8	250	2,45
	20	53,82	-52,3	320	1,52
	25	67,36	-66,55	420	0,81
	30	87,84	-87,65	650	0,19
b)	$h * 10^6, \text{cm}$	$B_1, \%$	$B_2, \%$	N_n	$B_3, \%$
	10	48,3	-46,5	340	1,8
	12	57,76	-56,62	380	1,14
	14	68,95	-68,24	500	0,71
	16	84,5	-84,24	610	0,26
c)	$h * 10^7, \text{cm}$	$B_1, \%$	$B_2, \%$	N_n	$B_3, \%$
	10	16,4	-11,7	180	4,7
	15	22,6	-19,3	250	3,3
	20	29,2	-26,7	280	2,5
	25	36,1	-34,2	330	1,9
	30	43,55	-42,1	400	1,45
	35	51,6	-50,5	480	1,1

Table 5. Dependence the percentage of the shift of the left and right boundaries of the region of result from the depth of penetration for gold in silicon: a) $E_0=1000$ keV; b) $E_0 = 500$ keV; c) $E_0 = 100$ keV

a)	$h * 10^4, \text{cm}$	$h/\lambda, \text{cm}$	$C_1, \%$	$C_2, \%$	N_h	$C_3, \%$
	1	161053	-8,035	11	530	2,965
	3	728805	-22,965	24,15	1500	1,185
	5	1895427	-31,53	32,1	3300	0,57
	7	4551380	-32,804	33,01	10000	0,206
	9	13087291	-21,27	21,287	100000	0,017
b)	$h * 10^4, \text{cm}$	$h/\lambda, \text{cm}$	$C_1, \%$	$C_2, \%$	N_h	$C_3, \%$
	1	419385	-14,16	15,85	1000	1,69
	2	1204988	-25,5	26,35	2100	0,85
	3	2729393	-32,0515	32,48	4500	0,4285
	4	6129971	-31,495	31,64	13500	0,145
5	17339549	-18,4049	18,4125	230000	0,0076	
c)	$h * 10^4, \text{cm}$	$h/\lambda, \text{cm}$	$C_1, \%$	$C_2, \%$	N_h	$C_3, \%$
	1	200374	-2,82	5,6	550	2,78
	3	717637	-11,36	12,75	1200	1,39
	5	1451482	-18,865	19,765	1950	0,9
	7	2523517	-25,265	25,860	3100	0,595
9	4167361	-29,8925	30,26	5200	0,3675	

Table 6. Dependence of the percentage of the shift of the left and right boundaries of the region of result on the depth of penetration for gold in gold at $E_0 = 100$ keV

$h * 10^6, \text{cm}$	$h/\lambda, \text{cm}$	$C_1, \%$	$C_2, \%$	N_h	$C_3, \%$
1,0	57721	-11,45	16,5	330	5,05
1,5	102546	-18,29	21,67	500	3,38
2,0	164619	-24,08	26,5	750	2,42
2,5	253442	-28,5708	30,1	1200	1,5292
3,0	387068	-31,13	32,17	1750	1,04
3,5	604507	-30,722	31,25	3700	0,528

The regularities of behavior of area of result depending on depth of penetration are revealed:

1. Depending on number of interactions the area is displaced to the right and narrowed, the left and right borders of area decrease, on the end of run sharply increase. At small values of initial energy slightly increase or decrease.
2. Depending on initial energy of a particle the area also is displaced to the right and narrowed.
3. With an increase of number of interactions the step for calculation strongly increases.

The irradiation of metals by heavy ions, to which correspond the higher densities, the defects are formed: vacancies type dislocation loops. In this case [9] it is assumed that the interstitial atoms migrate from the formed defective zone and the zones of vacancies remained in the atom athermally and thermally are reconstructed and collapse into the vacancies loop. Let us note that collapsing defective zone into the amorphous in the semiconductors and vacancies loop in the metals reflects different effectiveness of the migration of point defects, and influence of the type of interatomic bonds. Thus, existing works and existing methods of calculation of concentration of the defects arising at an irradiation of metals by fast ions, or essentially overestimate experimental data on concentration and do not explain their observable sizes, or in the offered models there are free parameters which are not defined from any physical reasons.

Let's consider process of formation of defects and vacancies clusters within the limits of CP - models for this purpose: first, we shall calculate power spectrum of primarily knocked-on atoms $W(E_0, E_2, h)$ on various depths. Secondly, knowing the $W(E_0, E_2, h)$, we shall find concentration of cascade areas. For calculation of vacancies clusters concentration it is necessary to integrate spectrum PBA $W(E_0, E_2, h)$ on E_2 from E_c up to E_{2max} [10,11]:

$$C_k(E_0, h) = \int_{E_c}^{E_{2max}} W(E_0, E_2, h) dE_2, \quad (8)$$

$$E_{2max} = \frac{4m_1c^2m_2c^2}{(m_1c^2 + m_2c^2)^2} E_1. \quad (9)$$

Spectrum of PBA $W(E_0, E_2, h)$ is determined by formula [10]:

$$W(E_0, E_2, h) = \sum_{n=0}^{n_1} \int_{h-k\lambda_2}^h \psi_n(h') \exp\left(-\frac{h-h'}{\lambda_2}\right) \frac{\omega(E_1, E_2, h') dh'}{\lambda_1(h') \lambda_2}, \quad (10)$$

where n_1 - the maximal number of elastic impacts, $\psi_n(h')$ - cascade-probabilistic function in view of losses of energy for ions after n-th of interactions on depth of generation h' . For finding λ_2 we calculate σ_2 from Rutherford's formula. In the elementary action at the depth of h' the PBA spectrum is defined as the ratio of differential Rutherford section to the integral, i.e. [12]:

$$w(E_1, E_2) = \frac{d\sigma(E_1, E_2)/dE_2}{\sigma(E_1)}, \quad (11)$$

$$\frac{d\sigma(E_1, E_2, h)}{dE_2} = 4\pi a_0^2 E_r^2 z_1^2 z_2^2 \frac{1}{E_1 E_2^2} 10^{24}. \quad (12)$$

Finally, we receive the formula for calculation vacancies clusters [13]:

$$C_k(E_0, h) = \frac{E_d (E_{2max} - E_c)}{E_c (E_{2max} - E_d)} \sum_{n=n_0}^{n_1} \int_{h-k\lambda_2}^h \psi_n(h') \exp\left(-\frac{h-h'}{\lambda_2}\right) \frac{dh'}{\lambda_1(h') \lambda_2}. \quad (13)$$

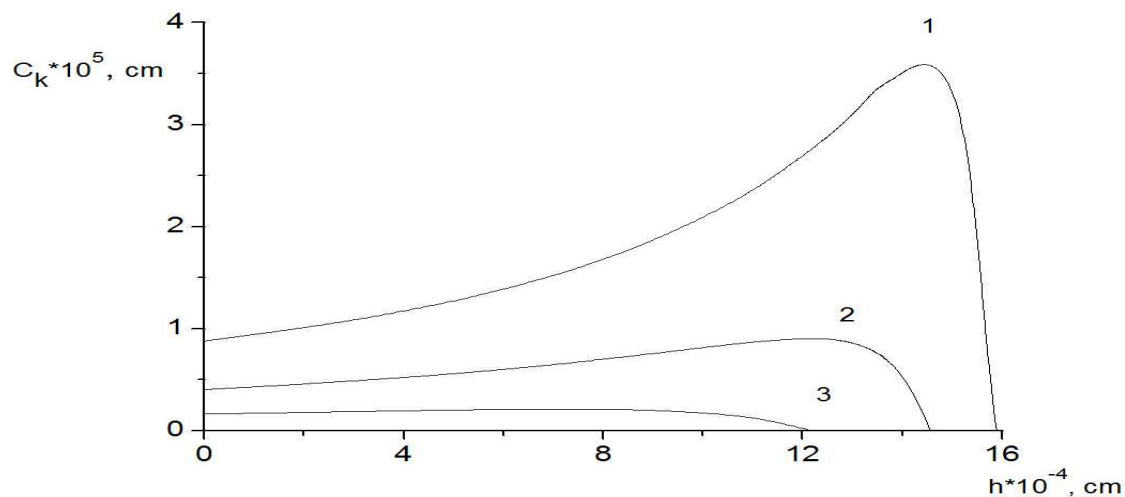


Fig. 5. Dependence of concentration of radiating defects on depth at an irradiation of silicon with ions of silver at $E_0 = 1000$ keV, $E_c = 50$ keV (1), 100 keV (2), 200 keV (3).

Table 7. Range borders of concentration definition of radiating defects for silver in silicon at $E_c = 50$ keV, $E_0 = 1000$ keV

$h * 10^4, \text{cm}$	C_k, cm	E_0, keV	n_0	n_1	τ
0,1	88082,9	1000	174	417	4''
1,81	99324,6	900	60299	63742	15'
3,60	113195,6	800	130090	135256	46'
5,37	130454,8	700	210534	217106	1°33'09''
7,11	152649,5	600	304159	311851	2°37'
8,84	181910,5	500	416958	426047	4°11'
10,52	220917,3	400	553995	564515	6°25'58''
11,35	246186,7	350	636131	647055	7°39'
12,17	275726,9	300	730486	742372	9°33'
12,50	288048,2	280	773157	785169	10°13'
12,82	301953,9	260	817668	830230	11°16'
13,14	327040,8	240	865743	878584	12°13'
13,47	345536,9	220	919681	932919	13°55'
13,79	343932,4	200	976991	991171	14°20'
14,11	354807,8	180	1040229	1054285	15°31'
14,43	360602,6	160	1110714	1125270	16°28'
14,74	355618,9	140	1187615	1202706	20°35'
15,07	330194,8	120	1281471	1297282	1, 5 d
15,39	254778,6	100	1388250	1404749	1, 7 d
15,72	61259,9	80	1521343	1538931	1, 8 d
15,89	0	70	1602632	1620512	2 d

Table 8. Range borders of concentration definition of radiating defects for silver in silicon at $E_c = 100$ keV, $E_0 = 1000$ keV

$h * 10^4, \text{cm}$	C_k, cm	E_0, keV	n_0	n_1	τ
0,1	40402,9	1000	174	417	4''
1,81	45061,29	900	60299	63742	15'
3,60	50629,54	800	130090	135256	46'
5,37	57246,47	700	210534	217106	1°33'
7,11	65202,7	600	304159	311851	2°36'
8,84	74573	500	416958	426047	4°11'
10,52	84417,19	400	553995	564515	6°26'01''
11,35	88771,47	350	636131	647055	7°39'
12,17	90830,92	300	730486	742372	9°33'
12,50	90065,35	280	773157	785169	10°13'
12,82	88254,7	260	817668	830230	11°16'
13,14	84265,7	240	865743	878584	12°13'
13,47	77424,67	220	919681	932919	13°55'
13,79	65868,23	200	976991	991171	14°20'
14,11	46839,1	180	1040229	1054285	16°43'
14,43	15891,79	160	1110714	1125270	18°56'
14,74	0	140	1187615	1202706	20°35'

Table 9. Range borders of concentration definition of radiating defects for gold in silver at $E_c = 100$ keV and $E_0 = 200$ keV

$h * 10^5, \text{cm}$	C_k, cm	E_0, keV	n_0	n_1	τ
0,1	2185733,1	200	15644	18053	6'
0,2	2058358,7	180	33412	36880	14'
0,3	180627	160	52883	57218	29'
0,5	1488195,1	140	97458	103303	1°29'
0,7	723628	120	150932	158182	2°09'
0,9	-927446,4	100	215684	224336	3°26'

Table 10. Range borders of concentration definition of radiating defects for copper in gold at $E_c = 200$ keV and $E_0 = 1000$ keV

$h * 10^5, \text{cm}$	C_k, cm	E_0, keV	n_0	n_1	τ
0,01	21580,5	1000	0	66	2''
0,6	22672,1	900	893	1507	10''
1,73	25345,3	800	2875	3908	1'
2,58	27323,0	700	4778	6085	1'
3,44	29141,5	600	7074	8647	2'
4,28	29802,4	500	9803	11642	3'
5,11	26816,5	400	13189	15312	5'
5,52	21741,9	350	15228	17505	7'
5,92	11135,3	300	17546	19988	7'
6,08	4234,8	280	18590	21102	9'
6,24	-5052	260	19715	22301	9'

Table 11. Range borders of concentration definition of radiating defects for gold in silver at $E_c = 50$ keV and $E_0 = 200$ keV

$h * 10^5, \text{cm}$	C_k, cm	E_0, keV	n_0	n_1	τ
0,1	7007867,7	200	15644	18053	7'
0,2	7302275,4	180	33412	36880	29'
0,3	7511692,1	160	52883	57218	46'
0,5	8284898,7	140	97458	103303	1°44'
0,7	8873991,1	120	150932	158182	3°
0,9	8996191,7	100	215684	224336	5°
1,1	7783588,7	80	295270	305387	5°18'
1,2	6039618,3	70	342258	352550	7°01'
1,3	2777112,7	60	395295	407000	10°06'
1,4	-3336586,8	50	455708	468109	9°52'

Table 12. Range borders of concentration definition of radiating defects for silver in silicon at $E_c = 50$ keV and $E_0 = 800$ keV

$h * 10^4, \text{cm}$	C_k, cm	E_0, keV	n_0	n_1	τ
0,01	107583,76	800	235	509	5''1
1,77	125089,72	700	75156	79064	20'38
3,51	147554,77	600	164969	170681	1°04'19''
5,24	177397,84	500	274346	281695	3°37'08''
6,92	217597,40	400	408428	417628	4°15'09''
7,75	242577,72	350	489277	498983	5°18'36''
8,57	273425,12	300	582509	592957	6°19'44''
8,9	286192,69	280	624780	635764	7°39'10''
9,22	299747,34	260	668937	680305	8°21'40''
9,54	313552,30	240	716695	728346	9°10'18''
9,87	329625,63	220	770351	782452	10°12'10''
10,19	342313,26	200	827439	840156	11°31'
10,51	354543,58	180	890512	903800	12°56'10''

Results of calculations are presented in figures 5 and in tables 7-12.

Behavior of concentration of vacancies clusters the following:

At $E = 50$ keV in the profiles appears the maximum, which indicates of localization of cascade regions at the small depth. With an increase of atom number of a target for the same flying particles value of function in a point of a maximum slightly increases, values of depths decrease, that is in heavier target vacancies congestions is formed more and in near-surface area. With an increase of initial energy of a particle the area of damage are displaced in depth of a material. At identical and for heavier particles on unit of a way of movement of the ion, it is formed more areas. With energies of flying particle at $E_0 = 100$ keV the maximum of function at a surface of a target, and its value is not enough and quickly vanishes, very small damaged area which lays within the limits of 10-100 nanometers consequently is formed. At carrying out of calculations there are the difficulties consisting in finding of result area: initial and final value of number of interactions n_0, n_1 . For the heavy flying particles and the heavy targets the count time is great and reaches several days.

The finding of result area of concentration of vacancies clusters at an ionic irradiation has allowed revealing the following regularities:

1. Depending on depth of penetration initial and final values of number of interactions increase, the interval of area of result (n_0, n_1) also increases and displaced to the right.
2. With reduction of initial energy of a primary particle the interval of result area is displaced to the right, values of concentration of radiating defects increase, values of depths of penetration decrease.
3. With an increase of atom number of a target the interval of result area significantly is displaced to the right and increases.
4. At the big atom weight of the flying particle and small targets the count time very strongly increases and reaches several hours and even days.
5. The values of concentration sharply grow with the large atomic weight of the flying particle and target, and increases the count time, in other respects the behavior of the region of result analogous.
6. At various values of threshold energy of border of result area remain former.
7. With an increase of threshold energy the values of concentration decrease, values of depths of penetration decreases.

Conclusion

Thus, the process of interaction of heavy ions with solid in the work is considered. Easy and heavy elements have been taken as the target. On the offered algorithms are carried out the calculations of cascade-probabilistic functions, spectrums of primarily knocked-on atoms, concentration of radiating defects. The results of calculations are presented in the form of graphs and tables. New regularities of CPF behavior, PKA spectrums, and concentration of vacancies cluster are received.

Received data attest, that concentration of cascade areas is very sensitive function to variations of initial energy of the flying particle, threshold energy on formation of the cascade, to atom weight of the target, to approximation parameters.

Experts on the radiating physics of the solid, positron physics, astrophysics, applied mathematics, can use the received models, algorithms and results of calculations.

References

1. Kupchishin A.A., Kupchishin A.I., Shmygaleva T.A., etc. Modeling on the PC and experimental researches of radiating processes in iron and firm alloys. - Almaty KazNAU, PTC, Open Company «KAMA», p. 263 (2010)

2. Kupchishin A.A., Kupchishin A.I., Shmygaleva T.A., etc. Radiating effects in titanic alloys and composites. Monograph. Almaty: Almaty KazNAU, Open Company «KAMA», Al-FarabiKazNU SRI of FTP. p.228 (2010)
3. Boos E.G., Kupchishin A.A., Kupchishin A.I., Shmygalev E.V., Shmygaleva T.A. Cascade-probabilistic method, the solution of radiation-physics tasks, equations of Boltzmann. Connection with the Markov chains. Monograph. Almaty.: Abay KazNPU, al-FarabiKazNU NII (Scientific Research Institute) NKHT and M. p. 388 (2015)
4. Kupchishin A.I., Komarov F.F, Shmygaleva T.A., Togambayeva A.K. Modeling of cascade areas in constructional materials // Materials science & technology conference and exhibition. (MS&T '08). David L.Lawrence Convention Center. Pittsburgh, Pennsylvania. October, 5-9, pp. 2183-2190 (2008)
5. Kupchishin A.I., Shmygaleva T.A., Komarov F.F, Togambayeva A.K. The Computation Modeling of the Cascade Areas in Solids // 2008 IEEE Nuclear Science Symposium & Medical Imaging Conference & 16th Room Temperature Semiconductor Detector Workshop. International Congress Center. Dresden, Germany 19-25 October. p.223
6. Kupchishin A.I., Shmygaleva T.A., Togambayeva A.K Mathematical modeling of cascade areas in constructional materials // Proceedings of The International Conference on Modelling and Simulation MS'08 Jordan. PETRA (Jordan), 18-20 November, 2008. p.115-119.
7. Kolmogorov A.N. The basic concepts of the probability theory, M.: Science, p.119 (1974)
8. Komarov F.F., Kumakhov M.A. and other. Tables of the parameters of the spatial distribution of the ion-implanted admixtures. Minsk: publishing house V.I. Lenin BGU, p.352 (1980)
9. Komarov F. F. Ionic implantation into the metals. - M, metallurgy, p. 216(1990)
10. Kupchishin A.A., Kupchishin A.I., Komarov F.F., Shmygaleva T.A., Togambaeva a. K. Computer simulation of radiation-physics processes in the materials, irradiated by light ions and their connection with the Markov processes // the transactions IV of international scientific conference “thermal radiation effects and processes in the inorganic materials. - Tomsk: Publ. TPU, pp. 405-408 (2004)
11. Kupchishin A.I., Kupchishin A.A., Shmygaleva T.A., Togambaeva a. K. Generation of radiation defects in the materials of those irradiated by light ions // nuclear and radiation physics: the materials of 4-th international conference, on September 15 to 17, 2003 ; the volume of the II. - Almaty: INP NNC of RK, pp. 134-139 (2004)
12. Boos E. G., Kupchishin A.I. Solution of physical problems by cascade- probabilistic method. - Alma Ata: Science,T.1., p.112 (1987)
13. Kupchishin A.A., Kupchishin A.I., Shmygaleva T.A. Application of cascade-probability technigue to processes of ion passage through matter. // Proc. Int. Conf. Application of accelerator in Research and Industry. Denton. Texas. USA,p.112 (1996)